

Superior decoy state and purification quantum key distribution protocols for realistic quantum-dot based single photon sources

Yoad Ordan*, Yuval Bloom*, Tamar Levin, Kfir Sulimany, and Ronen Rapaport†
Racah Institute of Physics, The Hebrew University of Jerusalem, Jerusalem 9190401, Israel

Jennifer A. Hollingsworth

*Materials Physics & Applications Division: Center for Integrated Nanotechnologies,
Los Alamos National Laboratory, Los Alamos, New Mexico 87545, USA*

(Dated: September 13, 2024)

The original proposal of quantum key distribution (QKD) was based on ideal single photon sources, which 40 years later, are still challenging to develop. Therefore, the development of decoy state protocols using weak coherent states (WCS) from lasers, set the frontier in terms of secure key rates. Here, we propose and experimentally emulate two simple-to-implement protocols that allow practical, far from ideal sub-Poissonian photon sources to outperform state-of-the-art WCS. By engineering the photon statistics of a quantum dot's biexciton-exciton cascade, we show that either a truncated decoy state protocol or a heralded purification protocol can be employed to achieve a significantly increased performance in terms of the maximal allowed channel loss for secure key creation, which can exceed that of WCS by more than 3dB. We then show that our recently demonstrated room temperature single photon sources, based on giant colloidal quantum dots coupled to nano-antennas, are already well within the optimal performance range. These protocols can be utilized efficiently on a host of various sub-Poissonian quantum emitters having controllable photon statistics, offering a practical approach to QKD without the hindering requirements on the single photon purity of the photon source.

I. INTRODUCTION

Quantum key distribution (QKD) stands as a prominent candidate for the post-quantum-computer secure optical communication, enabling a secure key-establishing protocol between two parties employing the quantum nature of light [1–3]. In theory, encoding the information for QKD onto pure single photon states, is ultimately secured. In practice, it is limited by imperfections of the transmitter and the receiver, making security proofs a challenging task [4, 5], thus reducing the maximal secure key rate (SKR) and the maximal losses in the communication channel over which SKR is achievable [6, 7].

One of the main practical limitations of QKD systems is the lack of an ideal source for single photons (SPS), required to prevent eavesdropping attacks such as photon number splitting attack (PNS) [8]. The SKR and maximal allowed channel loss (MCL) of simple QKD protocols decrease dramatically with the increase of two-or-more photon events being transmitted from the source [9, 10]. This leads to very stringent requirements on both the single photon purity and the photon emission rate of any practical SPS [11].

Despite many years of exploration and engineering [12, 13], a simple, stable SPS system that has the required aforementioned properties and can be employed in real-life QKD applications is still an outstanding challenge,

which led researchers to suggest and utilize protocols employing attenuated lasers emitting weak coherent states (WCS) [14]. As WCS has a Poissonian distribution of photons, and thus a two-or-more photons probability is never vanishing, advanced protocols such as decoy state protocols have been developed to enhance both SKR and MCL [11, 15–18].

Decoy state protocols introduce variations in the distribution of the emitted photons to better characterize the channel and obtain a tighter bound on the SKR [19–22], allowing detection of PNS attacks [23, 24]. Yet, even with decoy state protocols, WCS are highly sensitive [25, 26] to the high probability of the vacuum state, due to the dependence between the different photon number emission probabilities, which overall limits the possible SKR [9]. The above solutions and inherent limitations of WCS for QKD set clear opportunities for improving the security and efficiency of QKD applications using realistic SPS systems [27].

While efforts to develop a nearly ideal SPS are still ongoing by many groups [28–32], here we introduce a radically different, more realistic approach. By utilizing two new simple QKD protocols on compact, imperfect SPS sources, we significantly enhance the QKD performance, in terms of the MCL, as compared to even ideal, infinite decoy state protocols using WCS.

We base our protocols on our recent demonstrations of room temperature operating SPS devices based on a giant colloidal nanocrystal quantum dot (gCQD) coupled to a hybrid nanoantenna and plasmonic nanocone [33–37]. These SPS devices displayed a highly enhanced rate of photon emission approaching the GHz range, together with near-unity collection efficiencies ($> 90\%$) of

* These authors contributed equally to this work

† ronendr@phys.huji.ac.il

the emitted photons. The photon emission from such gCQDs is based on the bi-exciton (BX-X) emission cascade under optical excitation [38], and has been shown to be well described by a truncated photon-number Fock space with $N = 0, 1$, and 2 photons, with a negligible probability of $N > 2$ photons [39].

The two protocols are both based on our ability to vary and control the probabilities of emitting the different Fock states, $\{P_0, P_1, P_2\}$ over a wide range of values, by simply varying the optical excitation power. The first protocol we implement is a simple and realistic decoy state protocol for such a source. We show that with this new protocol, we can significantly exceed, by more than 3 dB, the MCL value of an ideal decoy state protocol using a WCS source. The second protocol uses an alternative approach based on heralded photon purification under saturated excitation. We show that a similar performance enhancement can also be achieved. Finally we experimentally verify that the probability for $N > 2$ ($P_{>2}$) is negligibly small, justifying our protocols' assumptions, and demonstrating that even existing SPS which are far from being ideal, can outperform the current state-of-the-art protocols based on WCS sources.

II. OPTICAL CONTROL OF PHOTON STATISTICS FROM THE BX-X EMISSION CASCADE IN A gCQD

Fig. 1a presents a schematic sketch of the BX-X cascade in a gCQD (see Supp. Sec. I) following a non-resonant pulse excitation with power I . Modelling this process, a BX state $|XX\rangle$ is excited by the absorption of *two pump photons*. This process happens with a probability:

$$P_{XX} = \frac{(\alpha I)^2}{1 + \alpha I + (\alpha I)^2}. \quad (1)$$

The probability of excitation of only the X state, $|X\rangle$, by the absorption of *only one pump photon*, is given by:

$$P_X = \frac{\alpha I}{1 + \alpha I + (\alpha I)^2}. \quad (2)$$

Here α is a constant related to the absorption cross-section of the gCQD and we assume that any larger excitonic complexes are negligible [39], as will be verified later in this paper.

Following an optical excitation, the biexciton state $|XX\rangle$ decays into a single exciton state $|X\rangle$ either radiatively, by emitting a single photon with a probability QY_{XX} , representing the BX quantum yield, or non-radiatively with a probability $1 - QY_{XX}$. The exciton state $|X\rangle$ can then recombine radiatively (non-radiatively) with probabilities QY_X , $(1 - QY_X)$, to the ground state such that the probability to emit zero, one

or two photons, defined as $\{P_0, P_1, P_2\}$ respectively, is:

$$P_1 = P_{XX}(QY_X + QY_{XX} - 2QY_XQY_{XX}) \quad (3)$$

$$+ P_XQY_X$$

$$P_2 = P_{XX}QY_XQY_{XX} \quad (4)$$

$$P_0 = 1 - P_1 - P_2 \quad (5)$$

Since P_{XX}, P_X depend on the excitation power, the probabilities to emit two, one or zero photons following excitation become excitation power dependent, allowing an external control over the emitted photon statistics as is required for decoy states protocols. Such a saturable behavior of the excitonic population allows us to define a relative excitation power $S = I/I_S$, where I_S is the saturation power, for which the detected count rate (which is linearly proportional to the average emission photon number) reaches 90% of the maximum value.

In Fig. 1(b), we experimentally demonstrate photon statistics control by varying the excitation power from a single bare gCQD. As S increases, the collected photon emission intensity increases sublinearly and saturates at $S \gtrsim 1$. A good fit of the theoretical model, based on the absorption probabilities given in Eqs. 1, 2 and on the subsequent emission probabilities QY_X, QY_{XX} is shown (see Supp. Sec. II). This fit confirms the basic assumptions given above for the BX-X cascade process.

At the same time, the measured second-order correlation function, $g^{(2)}(0)$, also increases in a similar manner. This is understood in the following way: at low powers, most emission events are empty as P_0 is the dominant term. As S increases, P_1 increases linearly (Eq. 2), while P_2 increases quadratically and thus is negligible at $S \ll 1$. Since $g^{(2)}(0)$ is an increasing function of $P_2/(\sum_{i=0,1,2} P_i)$, a saturable behavior of $g^{(2)}(0)$ with increasing S is also expected for $S \rightarrow 1$.

Importantly, as we also show experimentally, multi-excitonic emissions from the gCQD can be neglected due to their low emission probability [39], thus $P_{N>2} = 0$.

By measuring both $g^{(2)}(0)$ and the count-rate C , we can extract the probability distribution precisely, as is detailed in Supp. Sec. III.

In Fig. 1(c), we present the extracted photon emission probabilities $\{P_0, P_1, P_2\}$. As expected, the probability of emitting one or two photons increases with excitation power, but at a different rate, allowing optical control of the emitted photon statistics with only varying S .

III. QKD PROTOCOLS OUTPERFORMING WCS

After establishing the control of the different photon number probabilities, we now utilize this capability for two MCL-enhancing protocols, the first is a decoy-state protocol and the second is a heralded purification protocol.

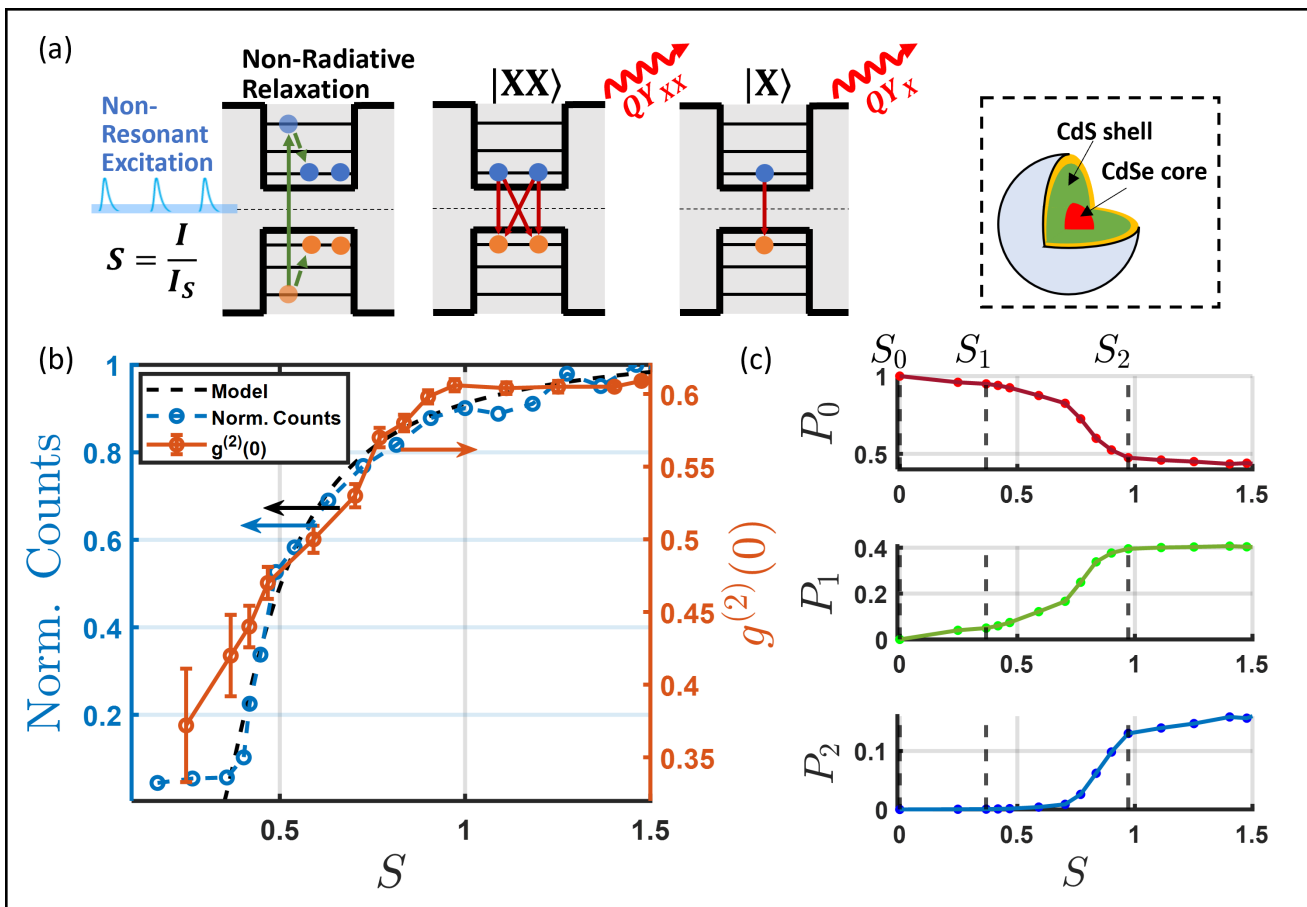


FIG. 1. (a) Schematic of the BX-X cascade in an optically excited gCQD, using a non-resonant pulsed excitation with a normalized intensity $S = \frac{I}{I_S}$. Inset is a sketch of a typical gCQD, consisting of a CdSe core and a CdS shell. (b) Normalized emission counts (blue open circles) as a function of S , displaying a saturation behaviour. The dashed black line is a fit to a model, detailed in Section II. The orange circles show the experimentally extracted $g^{(2)}(0)$ for the different powers. (c) Photon probabilities as a function of S . The dashed black lines mark the intensities chosen for the signal S_2 , and the two decoy states S_0, S_1 , for the decoy state on a truncated basis (DTB) protocol.

A. Decoy State on a Truncated Fock Basis - DTB

In Fig. 2(a), we present the conceptual experimental setup of the decoy state protocol. Here an SPS with a near unity photon collection efficiency, $\eta_c \simeq 1$ [36] (titled here SPS1), is used for implementing a BB84 protocol, but where Alice controls the excitation powers, $S_0 = 0$, S_1 and S_2 . This in turn modifies the photon number statistics, thus allowing for the implementation of decoy and signal states [11, 15].

To establish the DTB protocol, we define the gain of the signal (decoy_i), Q_s ($Q_{d,i}$), as the fraction of encoded photon pulses sent by Alice and detected by Bob. We also define the error rate of the signal (decoy_i), E_s ($E_{d,i}$), as the fraction of detected encoded photons that had errors. The signal pulses correspond to pulses with excitation S_2 , while the decoy pulses are those excited with S_1, S_0 . We show in the following that due to the truncated photon number basis of our SPS, only two different decoy states are enough for exact analysis in the framework of the

decoy state protocol [11].

Within the DTB protocol, Alice can randomly choose to replace the signal pulse with one of the two decoy states with different photon number distributions. These decoy states are not used to create the secure key but to improve the information about the channel and discover any possible eavesdroppers [15]. In the post-processing stage, Alice and Bob can verify the fraction of detected events and the errors for both signal pulses and decoy pulses, thus obtaining the gain and error rates $\{Q_s, Q_{d,i}, E_s, E_{d,i}\}$.

On the other hand, due to the uncertainty of the photon-number in each pulse, the gain and error rate for a specific n-photon state, $\{Q_n, e_n\}$, cannot be measured directly and have to be estimated or calculated. Out of this set, the single photon gain and error rate, Q_1, e_1 which are the probability of a detected event to originate from a single photon pulse and the error rate for single photon pulses respectively are of particular importance. This is since, considering a possible PNS attack by Eve,

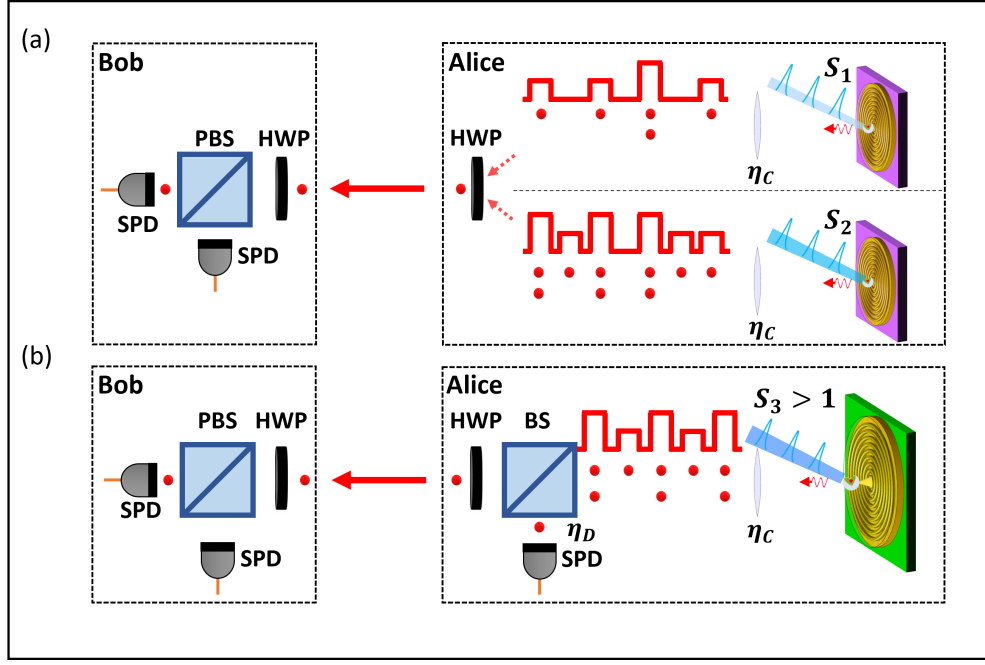


FIG. 2. Concept of two protocols based on a high rate, high collection efficiency SPS with imperfect purity: (a) Experimental setup and sketch of the BB84+DTB protocol, with Alice adjusting the excitation power on the SPS between $S_0 = 0$, S_1 and S_2 to control the emitted photon statistics for the 2-decoy protocol, followed by collection optics with efficiency η_C and a standard BB84 encoding unit. (b) Experimental setup and sketch of the BB84+HPP photon purification protocol. A single excitation power $S_3 > 1$, near saturation, is used to excite the SPS followed by collection optics with efficiency η_C and a beam-splitter (BS) with a high efficiency single photon detector with detection efficiency η_D . Here only same pulse detections at Alice and Bob are used for the secure key.

only information encoded on the single photon pulses is secured.

Crucially, in our three-intensity DTB protocol, these parameters can be solved exactly since the probability distribution of the signal and decoy states, $\{P_n^s\}, \{P_n^{d,i}\}$ is known, e.g. Fig. 1c. To relate the measured values $\{Q_s, Q_{d,i}, E_s, E_{d,i}\}$ to the unknown set $\{Q_n, e_n\}$, it is useful to define the n-photon yield, Y_n , as the conditional probability of a detection event given that Alice sent a n-photon state, and therefore $Q_n = Y_n P_n$. With these definitions, the following set of equations can be written [15]:

$$Q_s = \sum_{n=0}^2 P_n^s Y_n \quad E_s Q_s = \sum_{n=0}^2 P_n^s Y_n e_n \quad (6)$$

$$Q_{d,i} = \sum_{n=0}^2 P_n^{d,i} Y_n \quad E_{d,i} Q_{d,i} = \sum_{n=0}^2 P_n^{d,i} Y_n e_n \quad (7)$$

Importantly, unlike the decoy state protocol implemented for WCS where $n \rightarrow \infty$, and therefore require infinite set of decoy states for an exact solution [11], here $n = 0, 1, 2$ only. Thus, our equations have only six unknowns: $\{Y_0, e_0, Y_1, e_1, Y_2, e_2\}$ suggesting that two decoy states are enough for an exact solution to these equations. This makes the DTB implementation particularly viable, whereas for WCS using two decoy states would

only give a bounded approximation for the yield and errors [15].

The solution of these equations can then be used to estimate the minimum SKR after privacy amplification and error correction [11]:

$$SKR \geq q \{-Q_s f(E_s) H_2(E_s) + Q_1 [1 - H_2(e_1)]\} \quad (8)$$

where $q = 0.5$ for the BB84 protocol [1], H_2 is the binary Shannon information function [11] and $f(E_s)$ is the error correction efficiency (taken to be 1.22 [40]).

Assuming $\eta_C \simeq 1$ for gCQD on a nanoantenna [36] and using the probability values- P_0, P_1, P_2 , we can numerically calculate the SKR of such a source for different channel losses. For this, we use the channel model connecting the losses, yields, gains and the error-rates shown in [11] and in Supp. Sec. IV with the parameters values given in [41, 42], specifically, dark count probability of $P_{\text{dark}} = 1.7 \cdot 10^{-6}$, probability to reach the wrong detector of $e_d = 3.3\%$, Bob's detection efficiency of $\eta_{\text{Bob}} = 4.5\%$ and vacuum error-rate of $e_0 = 0.5$.

In Fig. 3(a) we show the calculated SKR under different channel losses for a standard WCS with decoy states (red) in the ideal, asymptotic case (infinite number of decoy states) with optimized intensity, compared to an SPS based on a gCQD coupled to a nanoantenna [36] (purple) using the above DTB protocol, with the realistically obtainable probabilities for such a device: $P_1^s = 0.529$,

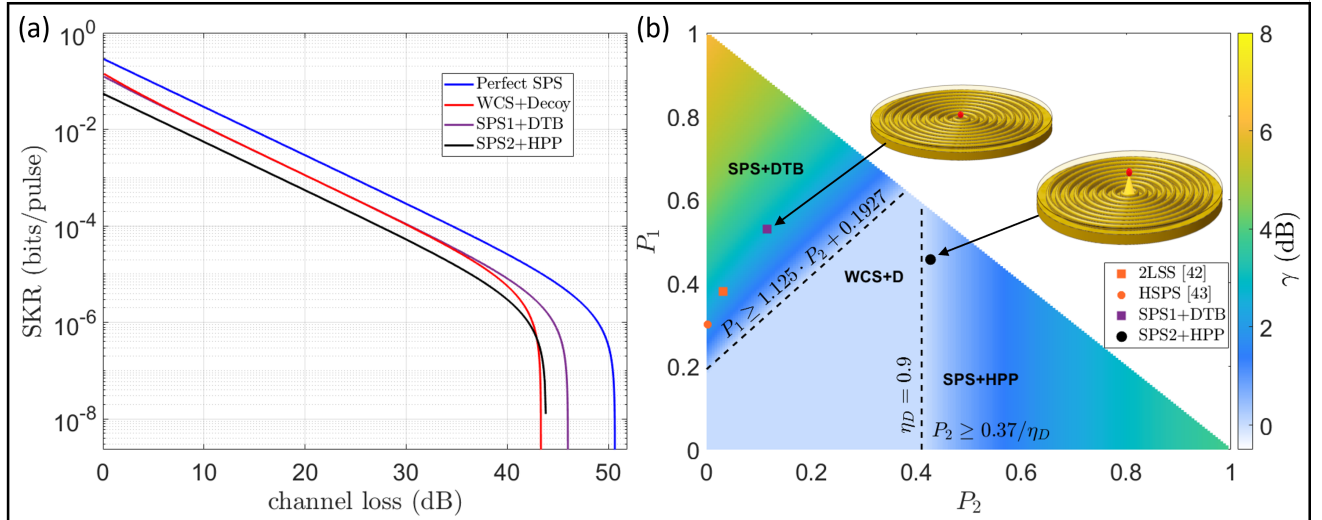


FIG. 3. **QKD analysis with imperfect single photon sources.** (a) Secure key rate of BB84 protocol as a function of channel loss for a perfect SPS (blue line), WCS with infinite decoy states and optimized intensities (WCS+Decoy, red), SPS1 with the decoy state on truncated basis protocol (SPS1+DTB, purple) and SPS2 with the heralded purification protocol (SPS2+HPP, black). The method and parameters of the calculations are found in Sec. III A and III B. (b) The relative gain of the MCL, γ , as a function of P_1, P_2 showing two advantageous regimes for SPS with either DTB or HPP separated by black dashed lines with their respective conditions. We also present our sources, SPS1 in the purification regime (black dot), SPS2 in the decoy state regime (purple square) and two, previously analyzed, non-classical sources [42, 43] marked with the orange square/dot.

$P_2^s = 0.112$ [36] for the signal state. A clear improvement in the SKR and the MCL of our imperfect SPS over WCS is seen, with over 3 dB MCL enhancement. We also show a comparison to a perfect single photon source ($P_1 = 1$) in black. Surprisingly, applying our truncated decoy-state protocol yields performance not far worse than a perfect SPS, even though our SPS is far from being ideal.

B. Heralded Purification Protocol- HPP

In Fig. 2(b), we present the experimental configuration of the heralded purification protocol (BB84+HPP). In this scheme, we consider a SPS consisting for example a gCQD on a hybrid nanocone-antenna device (titled here SPS2). Such a device showed both $\eta_C \simeq 1$ together with high attainable values of P_2 , resulting from a large Purcell factor induced by the nanocone which significantly enhances QY_{XX} [34, 44]. Alice operates at a single excitation power $S_3 > 1$, deep in the saturation regime, to excite the BX state with very high probability, thus maximizing P_2 , which is now only limited by QY_{XX} and QY_X [34]. A beam-splitter (BS) and a single photon detector (SPD) are added as a purification stage after the SPS in Alice's system, and before the standard BB84 encoding unit. As $P_{N>2}$ are negligible (see Supp. Sec. III), a real photon detection event in Alice's detector sets $\tilde{P}_2 = 0$ for that pulse, where \tilde{P}_n is the effective photon number probability after the purification stage. In the sifting step

of the QKD protocol, only events with same-pulse detections by Alice and Bob are considered for the secure key, thus eliminating all multiphoton events at a cost of lower signal rates.

Given a SPS having $\{P_0, P_1, P_2\}$, the effective distribution sent to Bob with HPP depends on the reflectance and transmission (R and T) of the BS and the detection efficiency of Alice's detector (η_D), as well as the probability of a dark count at Alice's detector (P_{DC}):

$$\tilde{P}_1 = 2P_2RT(\eta_D + P_{DC}) + TP_1P_{DC} \quad (9)$$

$$\tilde{P}_2 = T^2P_2P_{DC} \quad (10)$$

$$\tilde{P}_0 = 1 - \tilde{P}_1 - \tilde{P}_2 \quad (11)$$

Given this new distribution, we can again follow the well established method to estimate the SKR of a BB84 protocol (but now implemented with HPP) [11, 45]. The black line in Fig. 3(a) shows a realistic calculation of the SKR using actual parameters of SPS2 measured in Ref. [34]. A BS reflectance of 50% was chosen. We also used a SPD with $\eta_D = 0.9$ and $P_{DC} = 2 \cdot 10^{-7}$ corresponding to 100 dark counts per second for a 500 MHz signal rate which are both commonly attainable with current technology. Again, as is seen in the figure, the new BB84+HPP allows for a higher MCL (~ 1 dB) compared to WCS with infinite decoy, due to the extremely low \tilde{P}_2 . Remarkably, again this SKR enhancement can be achieved with SPS far from being ideal having a very low single photon purity.

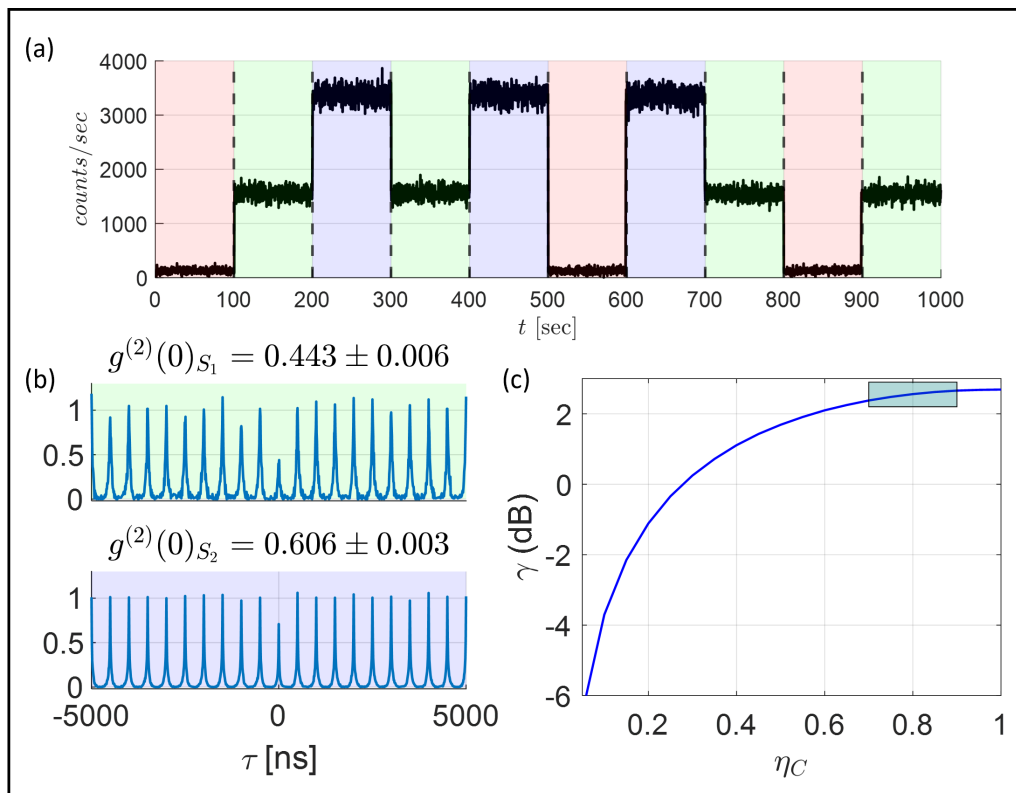


FIG. 4. **Experimental results for emulating the DTB protocol.** (a) Controlling the photon emission counts by the excitation laser intensity (405 nm, 2 MHz rep. rate, 2 ns pulse duration). Red regions mark S_0 , green regions mark S_1 and blue regions mark S_2 appearing in Fig. 1(c). (b) $g^{(2)}(0)$ for the two different intensities, S_1 , S_2 . (c) Calculation of γ values as a function of η_C . The blue box represents the η_C range demonstrated in our devices [34, 36], all with $\gamma > 2$ dB.

C. Performance Analysis

Next, we analyze the expected performance of realistic SPS-based BB84-QKD using the above protocols, in comparison to that of WCS with ideal decoy protocols. In particular, we compare the expected performance of our existing room-temperature high brightness, high collection efficiency SPS [34, 36]. We define the relative gain in the MCL as $\gamma = (MCL/MCL_{WCS})$, and use this parameter to evaluate the relative performance gain.

Fig. 3(b) shows a colormap of the calculated γ for different values of P_1, P_2 of the SPS (see Supp. Sec. IV). For high P_1 and sufficiently low P_2 , namely for $P_1 > 1.125P_2 + 0.1927$, there is a region (marked as "SPS+DTB") where $\gamma > 0$ dB, indicating that the use of an SPS with BB84+DTB protocol is advantageous over BB84 including decoy states with WCS (WCS+D). In this region, we highlight in orange dots two known non-classical sources [42, 43] along with our device (SPS1) consisting of a gCQD coupled to a metal-dielectric Bragg nanoantenna [36] (purple), demonstrating that already existing sources, when combined with the DTB protocol, can outperform even ideal WCS protocols. Notably, the use of DTB allows for SPS with a higher probability of two-photon events and shows that bright devices (with

fewer vacuum events) can be used for QKD even with single photon purities as low as $\sim 65\%$ and $g^{(2)}(0)$ values as high as ~ 0.6 .

On the other hand, for SPS with high enough values of P_2 , there is a region where BB84+HPP is advantageous over WCS+D, as shown in the right corner of Fig. 3(b) (marked as "SPS+HPP"), where $\gamma > 0$ dB. In the implementation of the HPP protocol, most one-photon events are discarded, and the key is composed largely of two-photon emission events, as indicated in Eq. 9, where the first term is dominant since $P_{DC} \ll P_1, P_2$. Therefore, the HPP method is most advantageous in the regime where P_2 is large, regardless of P_1 . The negligible probability of two-photon events after purification ($< 10^{-7}$) and minor contributions of the second and third terms in Eq. 9 result in an effectively pure source, differing from a perfect SPS only in brightness (through the zero-photon probability).

As indicated by the first term of Eq. 9, the probability of sending one photon is linearly dependent on η_D , suggesting that the minimum value of P_2 required for $\gamma > 0$ dB is inversely proportional to Alice's detection efficiency. Calculations yield this relation, giving the condition $P_2 \geq 0.37/\eta_D$ for a balanced 50:50 BS. The values of γ and the separation line between the WCS

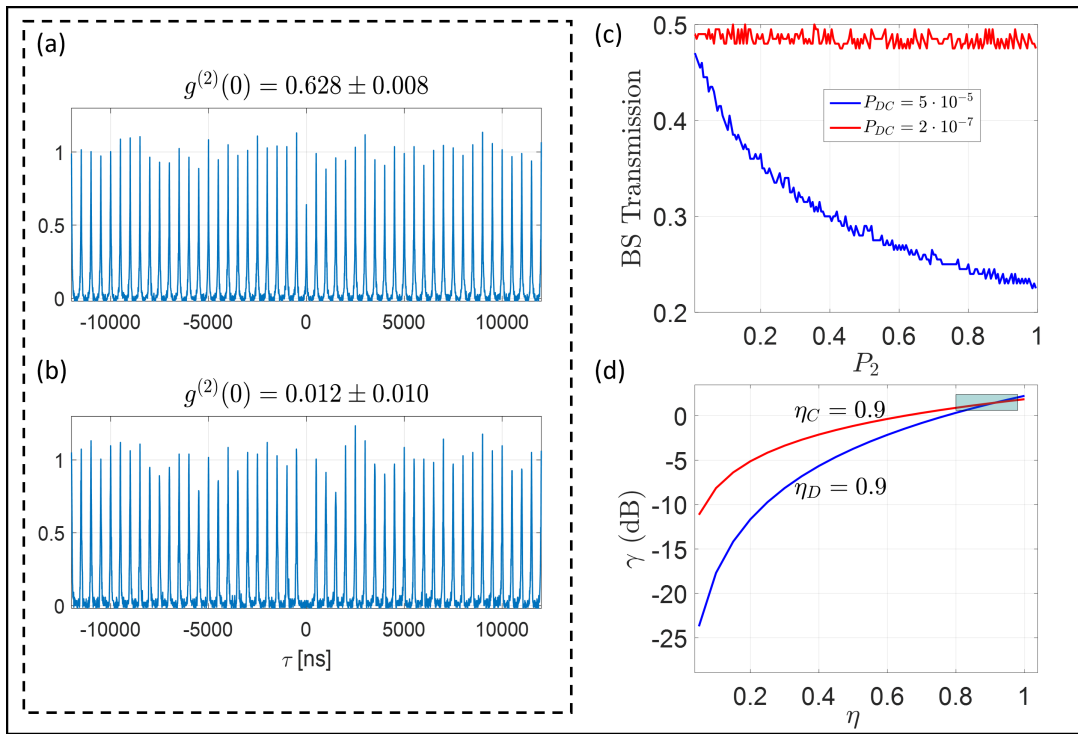


FIG. 5. **Experimental results for emulating the HPP protocol.** Second-order correlation measurements of the bare gCQD SPS without (a) and with (b) HPP post-processing scheme, resulting in near-zero $g^{(2)}(0)$. The error is mainly due to the SPD dark noise. (c) Calculation showing the optimal transmission T , of Alice’s BS, required for maximizing γ as a function of P_2 of the SPS, for two values of P_{DC} , corresponding to 100 dark counts per second of the SPD, and SPS excitation repetition rates of 2 (blue) and 500 (red) MHz. (d) Calculation of γ as a function of η_C with a fixed η_D (blue line) and as a function of η_D with a fixed η_C (red line). The blue box represents the range demonstrated in our devices [34, 36].

and HPP in Fig. 3(b) are evaluated for the realistic case $\eta_D = 0.9$, yielding an expected enhancement over WCS when $P_2 > 0.41$.

The black dot in Fig. 3(b) represents an actual SPS device consisting of a gCQD coupled to a Bragg antenna with a plasmonic nanocone (SPS2), demonstrated in Ref. [34], again showing that existing imperfect SPS+HPP can compete with WCS+D.

IV. EXPERIMENTAL RESULTS

After showing that existing SPSs, combined with the two new protocols can outperform WCS in terms of MCL, here we demonstrate experimental proof-of-concept emulations of both protocols using our bare single gCQD presented in Fig. 1(c) as our imperfect SPS emulator.

To experimentally demonstrate the feasibility of the DTB scheme, we use three different pulsed excitation intensities generated by a 405 nm diode laser, marked as $S_0 = 0$, S_1 , and S_2 in Fig. 1(c) (see Supp. Sec. V). Fig. 4(a) demonstrates photon emission control showing stable photon counts under each excitation intensity. This allows an easy control of the photon statistics, as shown in Fig. 4(b), which presents the $g^{(2)}(0)$ values for S_1 and S_2 , consistent with the modification of photon statistics

shown in Fig. 1, where $P_1^{(S_1)} = 0.05$, $P_1^{(S_2)} = 0.4$ and $P_2^{(S_1)} = 0.0005$, $P_2^{(S_2)} = 0.15$.

As shown previously, the gCQD SPS with a near unity collection efficiency can outperform WCS+D, if implemented with the DTB protocol. In Fig. 4(c), we numerically calculate the expected γ of a gCQD SPS device in terms of η_C (see Supp. Sec. VI). Remarkably, with the current measured parameters, $\gamma > 0$ dB already for $\eta_C > 0.3$, which is well within reach. As an example, our previously demonstrated gCQD based SPS devices [36] has $\eta_C > 0.7$ (marked by a blue rectangle) leading to an expected $\gamma > 2$ dB, a significant improvement over WCS+D.

Moving to emulation of the HPP protocol, we show experimental results of the purification of the gCQD emission in Fig. 5 (see Supp. Sec. V), using a 50:50 BS. The second-order correlation measurements of the gCQD without (Fig. 5(a)) and with (Fig. 5(b)) the HPP post-processing protocol are presented. As can be seen, a near-zero $g^{(2)}(0)$, limited only by detector noise is achieved, competing with state-of-the-art demonstrations [32, 46]. We note that with HPP, the photon rate decreases to $\sim 0.5P_2\eta_D$, but the collection efficiency η_C is not affected.

Using the results in Fig. 5(a),(b), we find that $P_3 \sim 10^{-7}$, therefore we conclude that $P_{N>2}$ is negligible com-

paring to P_1 and P_2 (see Supp. Sec. III), justifying our initial assumptions.

Interestingly, the HPP efficiency can be optimized by adjusting T , R of Alice's BS, depending on P_2 of the source. In Fig. 5(c) we show a calculation of the optimal beam splitter (BS) transmission T to reach the highest MCL, as a function of P_2 , for two dark-counts probabilities P_{DC} . For low P_{DC} the optimal transmittance is roughly 0.5, however for higher values of P_{DC} , the optimal T is smaller than 0.5 and decreases with increasing two-photon probability, in order to minimize the probability for a dark count at Alices' detector simultaneously with two-photons transmission to Bob.

Lastly, in Fig. 5(d) we plot the calculated γ for a gCQD based SPS with the above parameters, as a function of η_D , for a fixed $\eta_C = 0.9$ (red line), and as a function of η_C for a fixed $\eta_D = 0.9$. Again, the blue box, representing demonstrated values of SPS devices based on gCQD coupled to nano-antennas, shows an improvement over WCS+D.

V. CONCLUSIONS

As an alternative to the very challenging push for nearly ideal SPS that is required to outperform the existing WCS protocols for QKD, we proposed and analyzed two simple-to-implement protocols that can allow for even far from ideal SPS, which are currently technologically ready, to beat the state-of-the-art performance

of weak coherent states with decoy protocols, achieving over > 3 dB enhancement in terms of the secure key rate.

The protocols are based on the simple ability to control the statistical distribution of the truncated photon number basis $\{|0\rangle, |1\rangle, |2\rangle\}$ of a QD BX-X cascaded emission, by varying the excitation power. We showed that depending on the possible attainable values of P_1 and P_2 , either a decoy state protocol, DTB, or an heralded purification protocol, HPP, can be employed to a non-ideal SPS.

This is a particularly attractive route for improving the performance of current QKD systems, as we have shown that even room temperature, on-chip, compact, and easily integrated SPS devices, such as those based on gCQD coupled to nano-antennas, are already well within the parameter range for superior performance over WCS with decoy states by employing either a DTB protocol or HPP. Both protocols have very simple requirements and their application is very general, thus we believe they can be employed efficiently on a vast range of sub-Poisson, quantum emitters, opening a practical and realistic way to implement novel photon sources with superior QKD performance, without the stringent requirements that hindered their practical integration into real-world QKD systems.

Our protocols, which improves QKD performance, could also enhance other quantum cryptography technologies. By improving eavesdropping detection, it could strengthen quantum secure direct communication [47], quantum secret sharing [48], and quantum secure computation [49]. These protocols offer versatile improvement across various quantum cryptographic applications.

-
- [1] P. W. Shor and J. Preskill, Simple Proof of Security of the BB84 Quantum Key Distribution Protocol, *Physical Review Letters* **85**, 441 (2000).
- [2] R. Alléaume, C. Branciard, J. Bouda, T. Debuisschert, M. Dianati, N. Gisin, M. Godfrey, P. Grangier, T. Länger, N. Lütkenhaus, C. Monyk, P. Painchault, M. Peev, A. Poppe, T. Pornin, J. Rarity, R. Renner, G. Ribordy, M. Rigidel, L. Salvail, A. Shields, H. Weinfurter, and A. Zeilinger, Using quantum key distribution for cryptographic purposes: A survey, *Theoretical Computer Science* **560**, 62 (2014).
- [3] S. Pirandola, S. Pirandola, U. L. Andersen, L. Banchi, M. Berta, D. Bunandar, R. Colbeck, D. Englund, T. Gehring, C. Lupo, C. Ottaviani, J. L. Pereira, M. Razavi, J. S. Shaari, J. S. Shaari, M. Tomamichel, M. Tomamichel, V. C. Usenko, G. Vallone, P. Villoresi, and P. Wallden, Advances in quantum cryptography, *Advances in Optics and Photonics*, Vol. 12, Issue 4, pp. 1012-1236 **12**, 1012 (2020).
- [4] H. P. Yuen, Problems of Security Proofs and Fundamental Limit on Key Generation Rate in Quantum Key Distribution, *arXiv* (2012).
- [5] H. K. Lo, M. Curty, and K. Tamaki, Secure quantum key distribution, *Nature Photonics* 2014 8:8 **8**, 595 (2014).
- [6] F. Xu, X. Ma, Q. Zhang, H. K. Lo, and J. W. Pan, Secure quantum key distribution with realistic devices, *Reviews of Modern Physics* **92**, 025002 (2020).
- [7] V. Scarani, H. Bechmann-Pasquinucci, N. J. Cerf, M. Dušek, N. Lütkenhaus, and M. Peev, The security of practical quantum key distribution, *Reviews of Modern Physics* **81**, 1301 (2009).
- [8] R. G. Pousa, D. K. L. Oi, and J. Jeffers, Comparison of non-decoy single-photon source and decoy weak coherent pulse in quantum key distribution, *arXiv* (2024).
- [9] R. D. Somma and R. J. Hughes, Security of decoy-state protocols for general photon-number-splitting attacks, *Physical Review A - Atomic, Molecular, and Optical Physics* **87**, 062330 (2013).
- [10] M. Pereira, M. Curty, and K. Tamaki, Quantum key distribution with flawed and leaky sources, *npj Quantum Information* 2019 5:1 **5**, 1 (2019).
- [11] H. K. Lo, X. Ma, and K. Chen, Decoy state quantum key distribution, *Physical Review Letters* **94**, 230504 (2005).
- [12] M. D. Eisaman, J. Fan, A. Migdall, and S. V. Polyakov, Invited Review Article: Single-photon sources and detectors, *Review of Scientific Instruments* **82**, 71101 (2011).
- [13] B. Lounis and M. Orrit, Single-photon sources, *Reports on Progress in Physics* **68**, 1129 (2005).
- [14] D. Stucki, N. Brunner, N. Gisin, V. Scarani, and H. Zbinden, Fast and simple one-way quantum key distribution, *Applied Physics Letters* **87** (2005).
- [15] X. Ma, B. Qi, Y. Zhao, and H. K. Lo, Practical decoy

- state for quantum key distribution, *Physical Review A - Atomic, Molecular, and Optical Physics* **72**, 012326 (2005).
- [16] N. T. Islam, C. C. W. Lim, C. Cahall, J. Kim, and D. J. Gauthier, Provably secure and high-rate quantum key distribution with time-bin qudits, *Science advances* **3**, e1701491 (2017).
- [17] S.-K. Liao, W.-Q. Cai, W.-Y. Liu, L. Zhang, Y. Li, J.-G. Ren, J. Yin, Q. Shen, Y. Cao, Z.-P. Li, *et al.*, Satellite-to-ground quantum key distribution, *Nature* **549**, 43 (2017).
- [18] K. Sulimany, G. Pelc, R. Dudkiewicz, S. Korenblit, H. S. Eisenberg, Y. Bromberg, and M. Ben-Or, High-dimensional coherent one-way quantum key distribution, *arXiv preprint arXiv:2105.04733* (2021).
- [19] C. H. Zhang, S. L. Luo, G. C. Guo, and Q. Wang, Approaching the ideal quantum key distribution with two-intensity decoy states, *Physical Review A - Atomic, Molecular, and Optical Physics* **92**, 022332 (2015).
- [20] S. H. Sun, M. Gao, C. Y. Li, and L. M. Liang, Practical decoy-state measurement-device-independent quantum key distribution, *Physical Review A* **87**, 052329 (2013).
- [21] C. C. W. Lim, M. Curty, N. Walenta, F. Xu, and H. Zbinden, Concise security bounds for practical decoy-state quantum key distribution, *Physical Review A - Atomic, Molecular, and Optical Physics* **89**, 022307 (2014).
- [22] B. Kraus, C. Branciard, and R. Renner, Security of quantum-key-distribution protocols using two-way classical communication or weak coherent pulses, *Physical Review A - Atomic, Molecular, and Optical Physics* **75**, 012316 (2007).
- [23] X. B. Wang, Beating the Photon-Number-Splitting Attack in Practical Quantum Cryptography, *Physical Review Letters* **94**, 230503 (2005).
- [24] G. J. Fan-Yuan, Z. H. Wang, S. Wang, Z. Q. Yin, W. Chen, D. Y. He, G. C. Guo, and Z. F. Han, Optimizing Decoy-State Protocols for Practical Quantum Key Distribution Systems, *Advanced Quantum Technologies* **4**, 2000131 (2021).
- [25] Y. Chen, C. Huang, Z. Chen, W. He, C. Zhang, S. Sun, and K. Wei, Experimental study of secure quantum key distribution with source and detection imperfections, *Physical Review A* **106**, 022614 (2022).
- [26] W. P. Grice and B. Qi, Quantum secret sharing using weak coherent states, *Physical Review A* **100**, 022339 (2019).
- [27] Y. Zhang, X. Ding, Y. Li, L. Zhang, Y.-P. Guo, G.-Q. Wang, Z. Ning, M.-C. Xu, R.-Z. Liu, J.-Y. Zhao, G.-Y. Zou, H. Wang, Y. Cao, Y.-M. He, C.-Z. Peng, Y.-H. Huo, S.-K. Liao, C.-Y. Lu, F. Xu, and J.-W. Pan, Experimental single-photon quantum key distribution surpassing the fundamental coherent-state rate limit, *arXiv preprint arXiv:2405.03377* (2024).
- [28] M. Bozzio, M. Vvytlecka, M. Cosacchi, C. Nawrath, T. Seidlmann, J. C. Loredó, S. L. Portalupi, V. M. Axt, P. Michler, and P. Walther, Enhancing quantum cryptography with quantum dot single-photon sources, *npj Quantum Information* **2022** 8:1 **8**, 1 (2022).
- [29] C. R. Kagan, L. C. Bassett, C. B. Murray, and S. M. Thompson, Colloidal Quantum Dots as Platforms for Quantum Information Science, *Chemical Reviews* **121**, 3186 (2021).
- [30] J.-H. Kim, T. Heindel, S. Reitzenstein, A. Rastelli, and N. Gregersen, Quantum dots for photonic quantum information technology, *Advances in Optics and Photonics*, Vol. 15, Issue 3, pp. 613-738 **15**, 613 (2023).
- [31] H. Qian, J. Sun, X. Lu, a. , P. Grangier, B. Sanders, J. Vuckovic, S. Zhi Xia, K. Li, S. Buckley, K. Rivoire, and J. Vučkovi, Engineered quantum dot single-photon sources, *Reports on Progress in Physics* **75**, 126503 (2012).
- [32] D. Nelson, S. Byun, J. Bullock, K. B. Crozier, and S. Kim, Colloidal quantum dots as single photon sources, *Journal of Materials Chemistry C* **12**, 5684 (2024).
- [33] A. Nazarov, Y. Bloom, B. Lubotzky, H. Abudayyeh, A. Mildner, L. Baldessarini, Y. Shemla, E. G. Bowes, M. Fleischer, J. A. Hollingsworth, and R. Rapaport, Ultrafast and highly collimated radially polarized photons from a colloidal quantum dot in a hybrid nanoantenna at room-temperature, *arXiv preprint arXiv:2405.03377* (2024).
- [34] H. Abudayyeh, A. Mildner, D. Liran, B. Lubotzky, L. Lüder, M. Fleischer, and R. Rapaport, Overcoming the Rate-Directionality Trade-off: A Room-Temperature Ultrabright Quantum Light Source, *ACS Nano* **15**, 17384 (2021).
- [35] B. Lubotzky, A. Nazarov, H. Abudayyeh, L. Antoniuk, N. Lettner, V. Agafonov, A. V. Bennett, S. Majumder, V. Chandrasekaran, E. G. Bowes, H. Htoon, J. A. Hollingsworth, A. Kubanek, and R. Rapaport, Room-Temperature Fiber-Coupled Single-Photon Sources based on Colloidal Quantum Dots and SiV Centers in Back-Excited Nanoantennas, *Nano Letters* **24**, 640 (2024).
- [36] H. Abudayyeh, B. Lubotzky, A. Blake, J. Wang, S. Majumder, Z. Hu, Y. Kim, H. Htoon, R. Bose, A. V. Malko, J. A. Hollingsworth, and R. Rapaport, Single photon sources with near unity collection efficiencies by deterministic placement of quantum dots in nanoantennas, *APL Photonics* **6** (2021).
- [37] D. Halevi, B. Lubotzky, K. Sulimany, E. G. Bowes, J. A. Hollingsworth, Y. Bromberg, and R. Rapaport, High-dimensional quantum key distribution using orbital angular momentum of single photons from a colloidal quantum dot at room temperature, *arXiv preprint arXiv:2405.03377* (2024).
- [38] B. Li, G. Zhang, Y. Zhang, C. Yang, W. Guo, Y. Peng, R. Chen, C. Qin, Y. Gao, J. Hu, R. Wu, J. Ma, H. Zhong, Y. Zheng, L. Xiao, and S. Jia, Biexciton dynamics in single colloidal cdse quantum dots, *The Journal of Physical Chemistry Letters* **11**, 10425 (2020).
- [39] H. Abudayyeh, B. Lubotzky, S. Majumder, J. A. Hollingsworth, and R. Rapaport, Purification of Single Photons by Temporal Heralding of Quantum Dot Sources, *ACS Photonics* **6**, 446 (2019).
- [40] G. Brassard, N. Lütkenhaus, T. Mor, and B. C. Sanders, Limitations on practical quantum cryptography, *Phys. Rev. Lett.* **85**, 1330 (2000).
- [41] C. Gobby, a. Yuan, and A. Shields, Quantum key distribution over 122 km of standard telecom fiber, *Applied Physics Letters* **84**, 3762 (2004).
- [42] D. J. Gauthier, H. Zheng, and H. U. Baranger, Decoy-state quantum key distribution with nonclassical light generated in a one-dimensional waveguide, *Optics Letters*, Vol. 38, Issue 5, pp. 622-624 **38**, 622 (2013).
- [43] Q. Wang, W. Chen, G. Xavier, M. Swillo, T. Zhang, S. Sauge, M. Tengner, Z. F. Han, G. C. Guo, and A. Karlsson, Experimental decoy-state quantum key dis-

- tribution with a sub-poissonian heralded single-photon source, *Physical Review Letters* **100**, 090501 (2008).
- [44] K. Matsuzaki, S. Vassant, H. W. Liu, A. Dutschke, B. Hoffmann, X. Chen, S. Christiansen, M. R. Buck, J. A. Hollingsworth, S. Götzinger, and V. Sandoghdar, Strong plasmonic enhancement of biexciton emission: controlled coupling of a single quantum dot to a gold nanocone antenna, *Scientific Reports* 2017 7:1 **7**, 1 (2017).
- [45] D. Gottesman, Hoi-Kwong Lo, N. Lutkenhaus, and J. Preskill, Security of quantum key distribution with imperfect devices, *International Symposium on Information Theory, 2004. ISIT 2004. Proceedings.* , 135 (2004).
- [46] N. Somaschi, V. Giesz, L. De Santis, J. Loredano, M. P. Almeida, G. Hornecker, S. L. Portalupi, T. Grange, C. Anton, J. Demory, *et al.*, Near-optimal single-photon sources in the solid state, *Nature Photonics* **10**, 340 (2016).
- [47] J.-Y. Hu, B. Yu, M.-Y. Jing, L.-T. Xiao, S.-T. Jia, G.-Q. Qin, and G.-L. Long, Experimental quantum secure direct communication with single photons, *Light: Science & Applications* **5**, e16144 (2016).
- [48] M. Hillery, V. Bužek, and A. Berthiaume, Quantum secret sharing, *Physical Review A* **59**, 1829 (1999).
- [49] K. Sulimany, S. K. Vadlamani, R. Hamerly, P. Iyengar, and D. Englund, Quantum-secure multiparty deep learning, *arXiv preprint arXiv:2408.05629* (2024).